analytical chemistry

Article

Cite This: Anal. Chem. 2019, 91, 5881−5887

pubs.acs.org/ac

Targeted Determination of Tissue Energy Status by LC-MS/MS

Xiaorong Fu,[†,‡] Stanisław Deja,[†,§] Blanka Kucejova,[†,∥] Joao A. G. Duarte,[†,∥] Jeffrey G. McDonald,[†,‡] and Shawn C. Burgess*[,†,∥]

[†]Center for Human Nutrition, [‡]Department of Molecular Genetics, [§]Department of Biochemistry, and [∥]Department of Pharmacology, The University of Texas Southwestern Medical Center, Dallas, Texas 75390, United States

Supporting Information

ABSTRACT: Intracellular nucleotides and acyl-CoAs are metabolites that are central to the regulation of energy metabolism. They set the cellular energy charge and redox state, act as allosteric regulators, modulate signaling and transcription factors, and thermodynamically activate substrates for oxidation or biosynthesis. Unfortunately, no method exists to simultaneously quantify these biomolecules in tissue extracts. A simple method was developed using ion-pairing reversed-phase high-performance liquid chromatography−electrospray-ionization tandem mass spectrometry (HPLC-ESI-MS/MS) to simultaneously quantify adenine nucleotides (AMP, ADP, and ATP), pyridine dinucleotides (NAD^+ and NADH), and short-chain acyl-CoAs (acetyl, malonyl, succinyl, and propionyl). Quantitative analysis of these molecules in mouse liver was achieved using stable-isotope-labeled internal standards. The method was extensively validated by determining the linearity, accuracy, repeatability, and assay stability. Biological responsiveness was confirmed in assays of liver tissue with variable durations of ischemia, which had substantial effects on tissue energy charge and redox state. We conclude that the method provides a simple, fast, and reliable approach to the simultaneous analysis of nucleotides and short-chain acyl-CoAs.

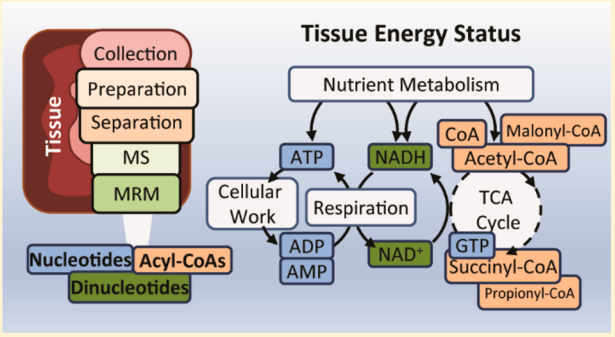

Adenosine nucleotides, nicotinamide adenine dinucleotides, and acyl-coenzyme A (CoA) are present in all living cells (Figure 1A). They are required as cofactors and units of basic energy transfer in metabolism. There are three adenosine nucleotides that have one, two, or three high-energy phosphates: adenosine 5′-monophate (AMP), adenosine 5′-diphosphate (ADP), and adenosine 5′-triphosphate (ATP). The hydrolysis of ATP to ADP and AMP is used to drive endergonic processes of metabolism. Collectively, they define cellular energy charge (EC), a measure of chemical energy available for metabolic processes. Nicotinamide adenine dinucleotide (NAD) exists in the oxidized (NAD^+) or reduced (NADH) form. NAD(H) is an essential cofactor for redox reactions in biochemistry and ultimately provides the H^+ gradient that drives respiration and ATP synthesis. Together, EC and the NAD^+/NADH ratio describe the energy status of biological systems and modify cell signaling through the AMPK and sirtuin pathways.[1,2]

Short-chain acyl-CoAs are also important indicators of energy status and function as regulators of downstream pathways that produce or utilize ATP. Acetyl-CoA is the product of β-oxidation and a substrate for the TCA cycle, both of which generate the NADH necessary for ATP production in the electron-transport chain. It is notable that acetyl-CoA also functions as a required allosteric activator of pyruvate carboxylase, which is the main anaplerotic pathway of the TCA cycle. Acetyl-CoA can be converted to malonyl-CoA by acetyl-CoA carboxylase, the first step in fatty acid and sterol synthesis. Malonyl-CoA also inhibits lipid oxidation by allosterically inhibiting carnitine palmitoyltransferase I activity. Therefore, quantification of nucleotides and short-chain acyl-CoAs is of great value for understanding the energetics and redox states of tissue (Figure 1A).

Despite their immense importance and closely related metabolic roles, the diverse chemical properties of these three classes of metabolites make them challenging to quantify in a unified analytical approach. First, adenosine nucleotides are extremely polar, rendering them weakly retained and poorly resolved by conventional reversed-phase high-performance liquid chromatography (RP-HPLC).[3,4] Approaches based on ion-pairing RP-HPLC have been developed for quantifying nucleotides in cell lysates,[5−9] some of which have been coupled with electrospray-ionization mass spectrometry (ESI-MS) using ion-pairing reagents such as trimethylamine (TEA), tetrabutylammonium acetate (TBAA), dibutylammonium formate (DBAF), and dimethylhexylamine (DMHA).[10−17] Hence, a general method could use this chromatographic approach. Second, universal extraction conditions are also difficult to identify. For example, NAD^+ is efficiently extracted from tissue by standard acid-extraction protocols, but NADH is unstable under those conditions[9,18,19] and is usually extracted with basic media.[20] Organic-solvent extraction

Received: January 12, 2019
Accepted: April 2, 2019
Published: April 2, 2019

DOI: 10.1021/acs.analchem.9b00217
Anal. Chem. 2019, 91, 5881−5887

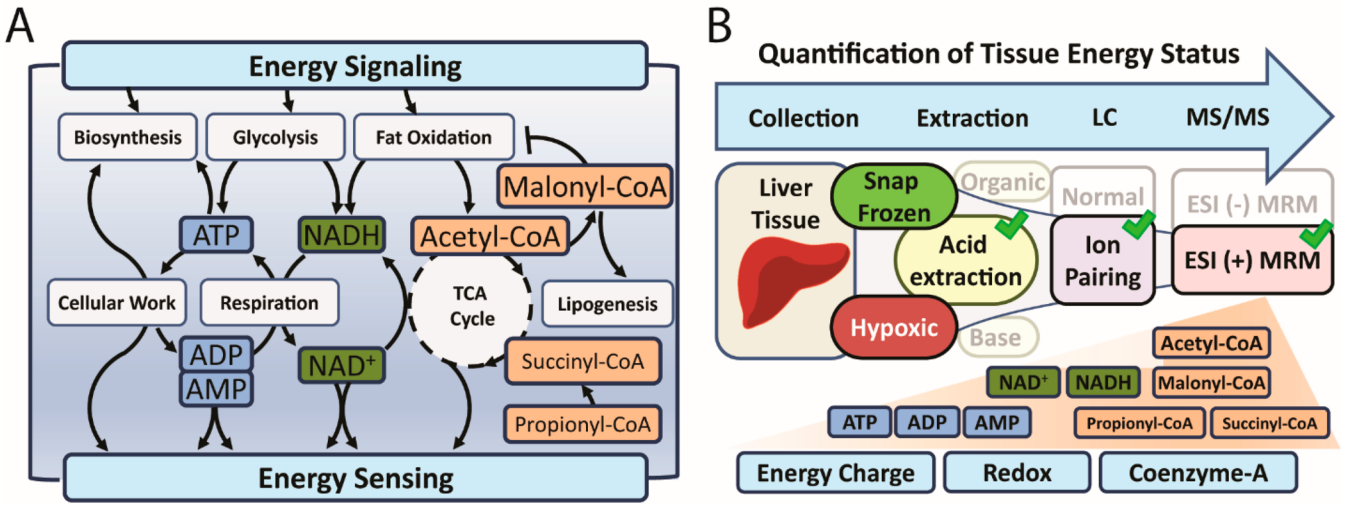

Figure 1. (A) General roles of adenosine phosphates, dinucleotides, and short-chain acyl-CoAs in metabolism and the energy status of liver. Nutrient oxidation in pathways like glycolysis and fat oxidation captures electrons by reducing NAD^+ to NADH. These pathways also generate acetyl-CoA, which is oxidized in the TCA cycle to generate more NADH. NADH is reoxidized to NAD^+ in the respiratory chain to drive ATP synthesis. The conversion of ATP to ADP and AMP supplies the free energy for multiple pathways of cellular work. Many of these metabolites can be sensed by regulatory proteins, such as AMPK and sirtuins, or allosterically modify enzymatic activity to signal for changes in flux through pathways of nutrient oxidation and biosynthesis. (B) Analytical methodology designed for the simultaneous quantification of adenosine phosphates, dinucleotides, and short-chain acyl-CoAs in tissue samples. Snap-freezing normoxic tissue ensures that physiological pools of metabolites are preserved. Acid extraction provides sufficient extraction efficiency for these classes of metabolites. Ion-pairing with DBAA provides sufficient chromatographic separation of these classes of metabolites. Positive MS/MS fragments were more efficient than negative-mode ones under these conditions.

protocols have been developed to simultaneously quantify NAD^+ and NADH,[18,19] but such approaches have poor yields for more polar adenosine nucleotides. It is known that NADH undergoes acid-catalyzed degradation to adenosine 5′-diphosphoribose (ADPR) during acid tissue extraction,[21−23] which could be used as a surrogate for NADH. Finally, tissue short-chain acyl-CoAs can be measured by GC-MS, but this approach requires careful derivatization[24] and is not amenable to the analysis of nucleotides. LC-MS methods have been developed to directly measure malonyl-CoA[25] and other short-chain acyl-CoAs in tissue by using $^{13}C_3$-malonyl-CoA and propionyl-CoA as internal standards.[26,27] However, these methods either do not utilize MS/MS for optimal specificity and sensitivity or lack specific internal standards. The challenge for a universal method will be to meet all requirements for each type of biological molecule.

We developed a general LC-MS/MS method (Figure 1B) based on volatile ion-pairing RP-HPLC, an NADH surrogate, and stable-isotope-labeled internal standards. We successfully quantified adenosine nucleotides (AMP, ADP, and ATP), nicotinamide adenine dinucleotides (NAD^+ and ADPR as a surrogate for NADH), and short-chain acyl-CoAs (acetyl-CoA, malonyl-CoA, succinyl-CoA, and propionyl-CoA). The method had excellent speed, sensitivity, and selectivity in a single analysis of liver tissue. We demonstrate that the method detects the rapid changes in energy and redox known to occur during the onset of ischemia−hypoxia in mouse liver. This method will be useful for researchers investigating tissue energetics using basic LC-MS/MS instrumentation.

MATERIALS AND METHODS

Chemicals and Materials. All nucleotides and coenzyme A standards, including adenosine 5′-triphosphate (ATP), adenosine 5′-diphosphate (ADP), adenosine 5′-monophosphate (AMP), β-nicotinamide adenine dinucleotide hydrate (NAD^+), β-nicotinamide adenine dinucleotide, reduced disodium salt hydrate (NADH), adenosine 5′-diphosphoribose (ADPR), acetyl coenzyme A (acetyl-CoA), malonyl coenzyme A (malonyl-CoA), succinyl coenzyme A (succinyl-CoA), and propionyl coenzyme A (propionyl-CoA), were purchased from Sigma (St. Louis, MO). Dibutylamine acetate (DBAA, 500 mM) solution was purchase from Sigma. HPLC-grade water, methanol, and acetonitrile were purchased from VWR (Radnor, PA). Internal standards (IS) [1,2-$^{13}C_2$] acetyl-CoA lithium salt, [1,2,3-$^{13}C_3$] malonyl-CoA lithium salt, [$^{13}C_{10}$,$^{15}N_5$] ATP sodium salt, and [$^{13}C_{10}$,$^{15}N_5$] AMP sodium salt were purchased from Sigma (St. Louis, MO).

Sample Preparation. Frozen liver samples were immediately spiked with stable-isotope-labeled ATP, AMP, acetyl-CoA, and malonyl-CoA internal standards. Approximately 50 mg of frozen tissue was homogenized in 500 μL of 0.4 M $HClO_4$ (PCA) containing 0.5 mM EGTA, and the tissue remained on ice for 10 min before being centrifuged at 14 000*g* at 4 °C for 10 min. The supernatant (400 μL) was neutralized with 135 μL of 0.5 M K_2CO_3, and the precipitate ($KClO_4$) was removed by centrifugation at 14 000*g* at 4 °C for 30 min. Neutralized supernatants were stored at −20 °C before being subjected to LC-MS/MS analyses.

Instrumentation. All experiments were carried out on a Shimadzu LC-20AD liquid chromatography (LC) system coupled to an API 3200 electrospray-ionization triple-quadrupole mass spectrometer (AB SCIEX, Framingham, MA). For initial investigation of the product spectrum of analytes (Figure 2), the standard solutions (1 μg/mL) were directly infused into the interface by a syringe pump. LC was performed on a reversed-phase C_{18} column (Waters xBridge, 150 × 2.1 mm, 3 μm). The standards and samples were separated using a mobile phase consisting of water/methanol (95:5, v/v) with 4 mM DBAA (eluent A) and water/acetonitrile (25:75, v/v; eluent B). The mobile phase was 0% B initially, which then increased

DOI: 10.1021/acs.analchem.9b00217
Anal. Chem. 2019, 91, 5881−5887

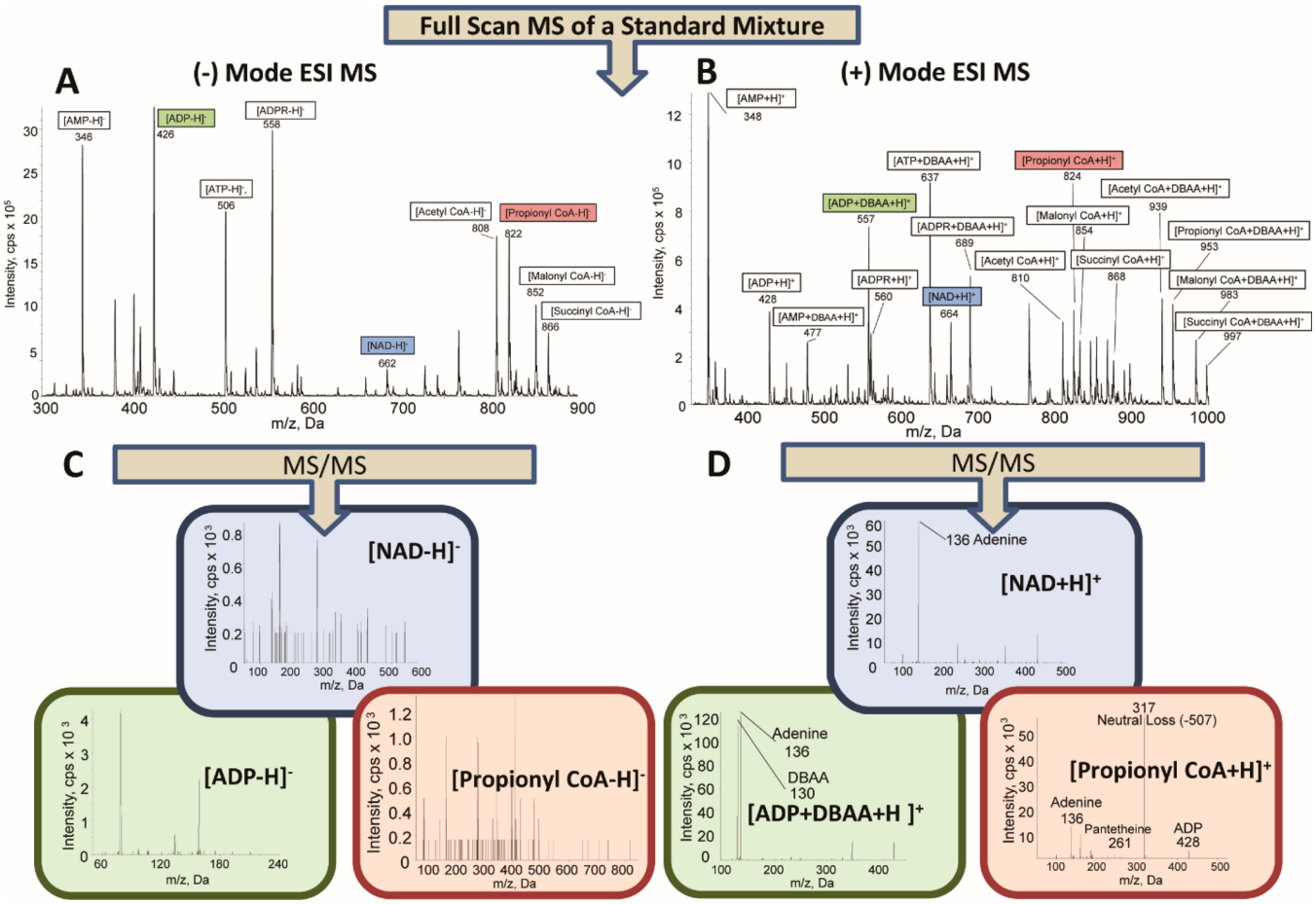

Figure 2. (A,B) MS full scan of a direct infusion of an analyte mixture with DBAA as the ion-pairing reagent in (A) negative-ion mode and (B) positive-ion mode. (C,D) Representative MS/MS spectra of ADP, NAD^+, and propionyl-CoA in (C) negative-ion mode and (D) positive-ion mode.

Table 1. Optimized MS Parameters in Positive-Ion-Mode MS[a]

analyte	molecular-ion structure	precursor/product transition of analyte	precursor/product transition of IS	DP (V)	EP (V)	CEP (V)	CE (V)	CXP (V)
ATP	$[ATP + DBAA + H]^+$	637/136	$[^{13}C_{10},^{15}N_5]$ ATP 652/146	55	5	25	65	3
ADP	$[ADP + DBAA + H]^+$	557/136	$[^{13}C_{10},^{15}N_5]$ ATP 652/146	25	3.6	20	48	3.1
AMP	$[AMP + DBAA + H]^+$	477/136	$[^{13}C_{10},^{15}N_5]$ AMP 492/146	14	2.2	24.5	36.8	3.4
NAD^+	$[NAD + H]^+$	664/136	$[^{13}C_{10},^{15}N_5]$ ATP 652/146	45	6.8	38	74	3.1
ADPR (NADH)	$[ADPR + DBAA + H]^+$	689/136	$[^{13}C_{10},^{15}N_5]$ ATP 652/146	49	6	42	55	8
acetyl-CoA	$[acetyl\text{-}CoA + H]^+$	810/303	$[1,2\text{-}^{13}C_2]$ acetyl-CoA 812/305	105	11	30	42	4.5
malonyl-CoA	$[malonyl\text{-}CoA + H]^+$	854/303	$[1,2,3\text{-}^{13}C_3]$ malonyl-CoA 857/305	90	11	53	57	6
succinyl-CoA	$[succinyl\text{-}CoA + H]^+$	868/361	$[1,2,3\text{-}^{13}C_3]$ malonyl-CoA 857/305	100	10	50	48	6
propionyl-CoA	$[propionyl\text{-}CoA + H]^+$	824/317	$[1,2,3\text{-}^{13}C_3]$ malonyl-CoA 857/305	100	10	27	47	4.8

[a]Stable-isotope-labeled AMP (transition 492/146), ATP (transition 652/146), acetyl-CoA (transition 812/305), and malonyl-CoA (transition 857/305) were used as internal standards.

to 80% over 8 min and then to 100% over 5 min. The mobile phase was held at 100% B for 3 min and then reequilibrated to 0% B and held for 5 min. The flow rate was 180 μL/min. A diverter valve was employed to reduce the introduction of

DOI: 10.1021/acs.analchem.9b00217
Anal. Chem. 2019, 91, 5881−5887

matrix components in the spectrometer. The mass spectra were acquired using electrospray ionization in positive-ion mode. Multiple-reaction monitoring (MRM) of MS/MS was used for the specific detection of each analyte and its stable isotope. The settings of the ESI source were as follows: 30 psi curtain gas, 3500 V ionization, 350 °C temperature, 30 psi nebulizer gas, and 40 psi heating gas. The mass spectrometer was set with a dwell time of 80 ms for the MRM-scan survey. The declustering (DP), entrance (EP), collision-energy (CE), and collision-cell-exit (CXP) potentials for each MRM transition of analytes and internal standards are reported in Table 1.

Optimization of Chromatographic Conditions. Retention times in ion-pairing chromatography were optimized by adjusting the concentration of the ion-pairing reagent as previously described.[14] We tested several concentrations of DBAA (1, 2, 4, 6, and 10 mM) in mobile phase A for optimal analyte separation (Figure S1).

Calibration, Quantification, and Validation. Stable-isotope-labeled AMP, ATP, acetyl-CoA, and malonyl-CoA were used as internal standards to control for extraction efficiency, MS response, variable LC retention times, and ionization efficiency. Isotopically labeled ATP was used to quantify ATP, ADP, NAD^+, and ADPR (NADH), whereas isotopically labeled malonyl-CoA was used to quantify malonyl-CoA, succinyl-CoA, and propionyl-CoA (Table 1). Standards of ATP, ADP, AMP, NAD^+, ADPR, short-chain acyl-CoAs, and stable-isotope-labeled internal standards were accurately weighed and dissolved in water to prepare stock solutions at 1.0 mg/mL. Calibration curves were constructed in the range of 10 ng/mL to 50 μg/mL with a fixed amount of stock solutions. Values for the slope, intercept, and correlation coefficient were obtained by linear-regression analysis of the calibration curves constructed by plotting analyte/internal-standard peak-area ratios versus concentrations (Table S1). The area under each analyte peak, relative to the internal standard, was quantified using Analyst software 1.7 (AB SCIEX) and used to calculate the analyte concentrations.

Method accuracy, precision, and repeatability and sample stability and recovery were determined in mouse liver tissue processed as described above with 200 μL aliquots distributed into microcentrifuge tubes and stored at −80 °C. The accuracy of the method was evaluated by recoveries of additional analyte added to liver-tissue samples. Stable-isotope-labeled AMP, ATP, acetyl-CoA, and malonyl-CoA internal standards and known amounts of analytes (0, 1.5, 4, and 6 μg in triplicate) were added to tissue homogenates (Table S2). Sample recovery is expressed as [(found amount − endogenous amount)/spiked amount × 100%]. The precision of the method was examined by triplicate analysis over 3 separate days (Table S3) and was estimated as the coefficient of variation (CV, %) of the replicate intra- and interday measurements, with a new standard curve each day. To assess extract stability, acidified liver extracts were spun, pooled, neutralized, and divided into multiple aliquots. One aliquot sample was analyzed immediately, whereas the rest were stored at room temperature, 4 °C, or −20 °C for 1, 4, 8, 19, or 28 days for subsequent analyses. Analyte stabilities in stored samples were compared to extracts stored at −80 °C prior to neutralization. The assay-stability profile was indicated by the fold-change of each analyte relative to immediate analysis.

The biological responsiveness of the method was demonstrated using liver tissue collected from overnight fasted male C57BL6J mice. Animal protocols were approved by the Institutional Animal Care and Use Committee at the University of Texas Southwestern Medical Center. Liver samples were collected from isoflurane anesthetized mice in situ either by dissecting and immediately freezing tissue (1 s) in liquid N_2 or by collecting ∼1 mL of blood from the descending aorta (inducing hypovolemic ischemia) and then dissecting and freezing the samples 27−270 s later. All samples were stored at −80 °C until analysis. Cellular energy charge was calculated as

$$EC = \frac{[ATP] + 0.5[ADP]}{[ATP] + [ADP] + [AMP]}$$

RESULTS AND DISCUSSION

Detection of Nucleotides and CoAs by MS/MS in Positive Mode after Ion-Pairing Liquid Chromatography. Adenosine nucleotides and short-chain acyl-CoAs have poor chromatographic retention under conventional reverse-phase conditions but can be separated using various ion-pairing reagents. Dibutylammonium acetate (DBAA) achieved better chromatographic separation than TEA or DMHA, which gave poor peak shapes for the analysis of nucleotides from liver extracts (Figure S2). As expected, the retention times tended to increase with higher DBAA concentrations for all the analytes (except for NAD^+, Figure S1A). Ion-pairing reagents can negatively affect ESI-MS detection, so we tested the effect of DBAA on the analysis of nucleotides and acyl-CoAs (Figure S1B). Although most analytes were only moderately affected, the ATP and ADP signals were significantly reduced with increasing DBAA concentration. Hence, we chose 4 mM DBAA, which was the lowest concentration that achieved good separation of ADPR from other coelutants. Methanol and acetonitrile were tested as mobile phase B. Acetonitrile was found to give better peak shapes (Figure S1C−K) with a shallow gradient and lower column back pressure.

To specifically evaluate the analysis of nucleotides and acyl-CoA species using DBBA as an ion-pairing reagent, we performed MS detection in both negative- and positive-ion modes (Figure 2). The use of negative-ion-mode ESI-MS is a logical approach for adenosine nucleotide detection because of the presence of up to three negatively charged phosphate groups.[14−16] Indeed, negative-ion full-scan mode provided relatively simple spectra with $[M - H]^-$ as the most prominent ion among all analytes (Figure 2A). However, positive-ion ESI-MS is known to have better sensitivity and an improved MS response compared with negative-ion mode when ion-pairing reagents are present.[28] Positive-ion ESI-MS has been successfully applied to the analysis of nucleosides, nucleotides,[28] and ribonucleotides.[13] An important advantage is that nucleotides form a unique and abundant product ion in positive-ion-mode LC-MS/MS.[17] Positive-ion-mode (Figure 2B), full-scan spectra were more complex than negative-ion-mode spectra. The AMP molecular ion $[AMP + H]^+$ (m/z 348) was ∼6 times higher than the $[AMP + DBAA + H]^+$ (m/z 477) adduct ion. However, with increasing numbers of negatively charged phosphate groups, such as in ADP, ADPR, and ATP, the efficiency of adduct-ion formation ($[M + DBAA + H]^+$) was greatly enhanced. This phenomenon was most striking for ATP, which has three negatively charged phosphate groups and produced $[ATP + DBAA + H]^+$ exclusively. In contrast, full-scan, positive-ion ESI-MS analysis of NAD^+ produced mostly $[NAD + H]^+$ (m/z 664) rather than [NAD

DOI: 10.1021/acs.analchem.9b00217
Anal. Chem. 2019, 91, 5881−5887

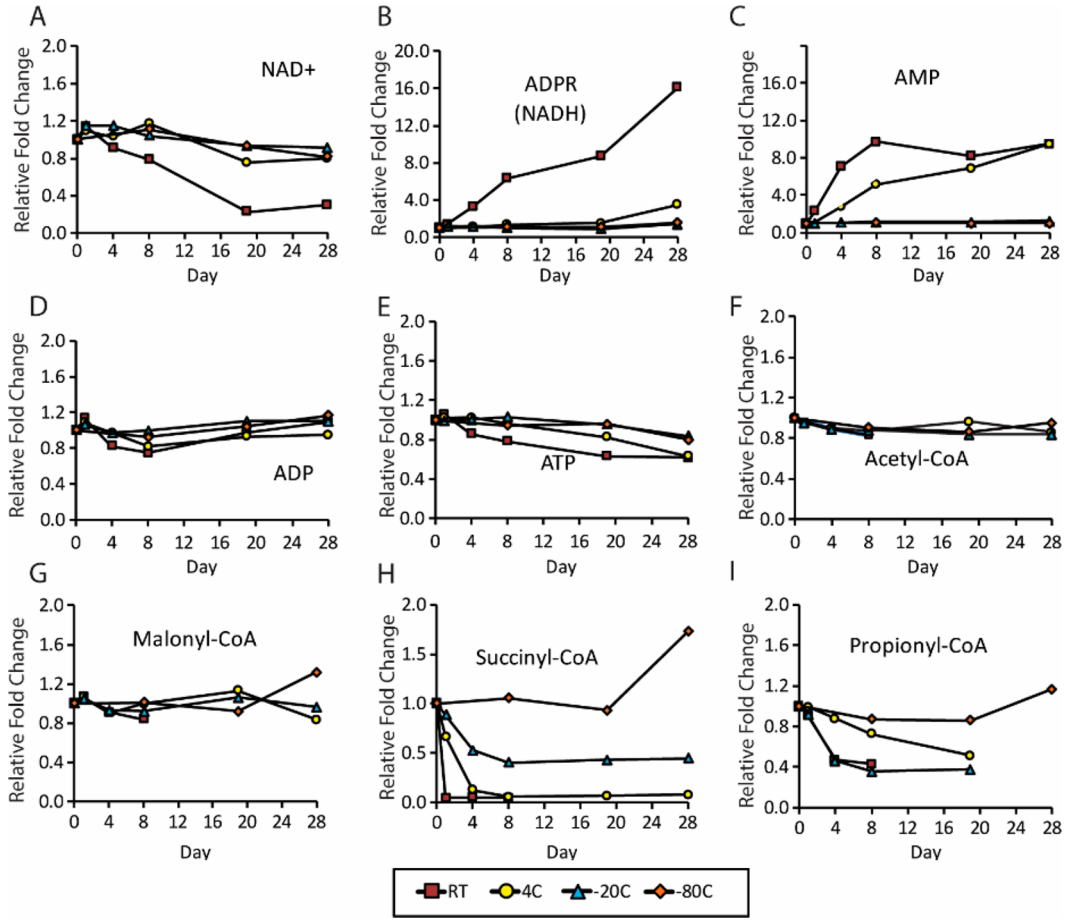

Figure 3. Assay stability using stable-isotope-labeled internal standards at room temperature, 4 °C, −20 °C, and −80 °C for (A) NAD^+, (B) ADPR (NADH), (C) AMP, (D) ADP, (E) ATP, (F) acetyl-CoA, (G) malonyl-CoA, (H) succinyl-CoA, and (I) propionyl-CoA. All analytes could be accurately quantified for 20 days when acidified liver extracts were stored at −80 °C.

+ DBAA + $H]^+$. Short-chain acyl-CoAs produced [M + DBAA + $H]^+$ and [M + $H]^+$ ions in near equal amounts. Overall, the intensities of [M − $H]^-$ ions in negative-ion mode were generally stronger than those observed for the [M + DBAA + $H]^+$ ion in positive-ion mode, likely because of the increased distribution of the total ion content in the latter.[14]

Despite weaker signals in positive-ion mode, the MS/MS product-ion spectra were much stronger than those from negative-ion mode for all analytes. For example, ADP, NAD^+, and propionyl-CoA are shown in Figure 2C,D. No significant fragment ions were detected for NAD^+ and propionyl-CoA under negative-ion mode (Figure 2C). Under positive-ion mode, the major collision-induced fragments of ADP at m/z 136 and 130 correspond to the fragmentation of the adenine base and DBA molecules, respectively (Figure 2D). Because short-chain acyl-CoAs form both protonated and adduct ions with similar intensity, MS/MS fragment species and their intensities were monitored for both molecule ions, which were found to be similar for all short-chain acyl-CoAs (data not shown). Short-chain acyl-CoAs produced abundant fragments, as previously reported.[27,29] The predominant MS/MS fragment was the acyl-pantetheine fragment, derived by a neutral loss of 507. Other fragments observed were 428 (ADP), 136 (adenine), and 261 (pantetheine). A compilation of analytes examined using this method, including the corresponding MS parameters, are shown in Table 1. Because of significantly higher MS/MS responses in positive-ion mode for the analytes, precursor ions and product ions were detected in ESI positive-ion mode, and quantification was performed in MRM mode. Detection of nucleotides and acyl-CoAs by ion-pairing LC-MS/MS resulted in excellent linearity ($r \geq 0.9994$) for all analytes (Table S1). We noted nonunity slopes for most analytes, indicating that individual calibration curves should be generated. Analyte recoveries ranged from 83.7 to 112.0%, and the CV of the method ranged from 0.5 to 13.9% (Table S2). The method had very good intra- and interday precision, with a CV less than 15% for all analytes except malonyl-CoA, which was 18.9% for the interday repeatability (Table S3).

Labile Nucleotide and Acyl-CoA Samples. Biological nucleotides and CoAs are inherently reactive and must be stored at low temperatures to minimize sample degradation.[30] Nearly all analytes degraded (>20%) when neutralized extracts were stored at room temperature for a single day (Figure S3). Nucleotides were protected for several days at 4 °C and several weeks at ≤−20 °C. CoAs were more labile than nucleotides and degraded within days of storage at ≤−20 °C or within 2 weeks when acidified extracts were stored at −80 °C (Figure S3). Fortunately, internal stable-isotope standards provided some analytical protection against analyte lability (Figure 3). Thus, nucleotides, acetyl-CoA, and malonyl-CoA (Figure 3A−G) could be quantified for at least 28 days when stored at ≤−20 °C with internal standards. However, because stable-isotope-labeled succinyl-CoA and propionyl-CoA were unavailable, even 1 day at −20 °C caused a 12% underestimation,

DOI: 10.1021/acs.analchem.9b00217
Anal. Chem. 2019, 91, 5881−5887

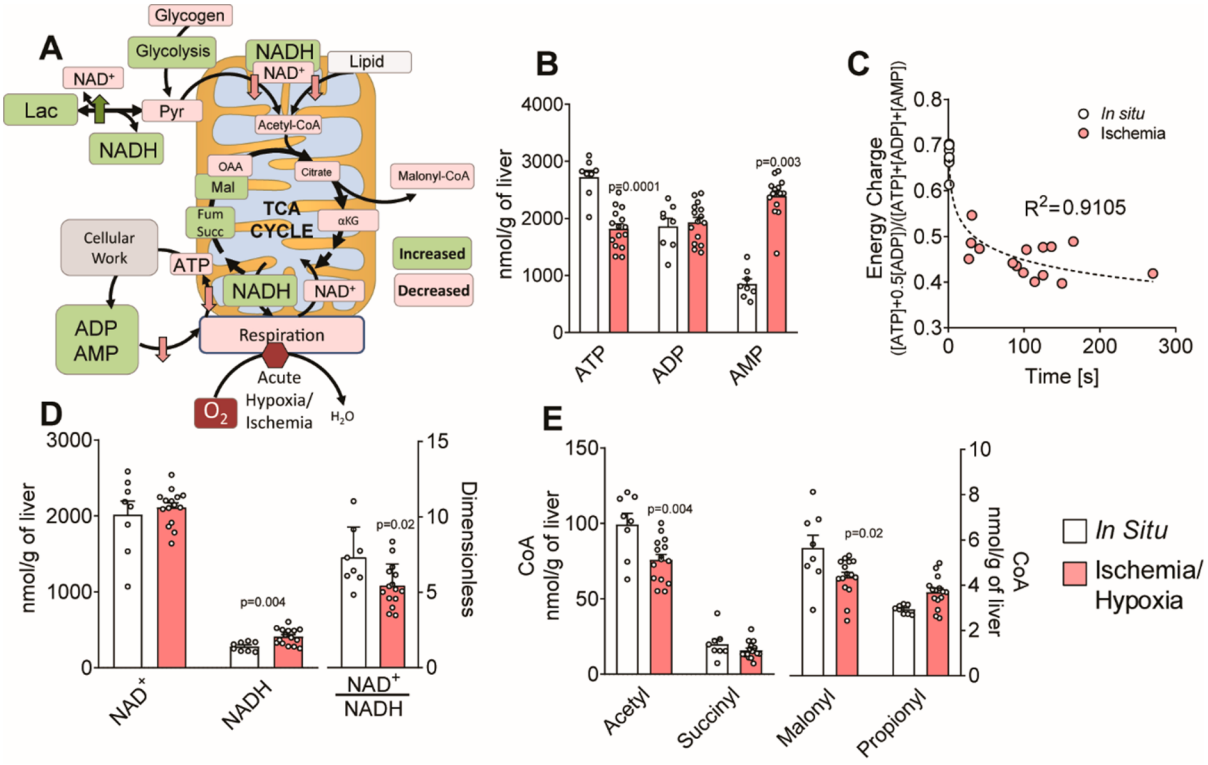

Figure 4. (A) Effect of hypoxia and ischemia on select metabolites and cofactors related to energy metabolism. Oxygen deficiency inhibits respiration, leading to an accumulation of NADH and lack of ATP. The resulting decrease in NAD^+/NADH inhibits the TCA cycle and fat oxidation, decreases associated acyl-CoAs, and stimulates anaerobic glycolysis. (B–E) Effect of elapsed time between large-volume blood draw (ischemia–hypoxia) and sample freezing on (B) liver nucleotides; (C) energy charge; (D) NAD^+, NADH, and NAD^+/NADH; and (E) short-chain acyl-CoAs.

and 4 days resulted in a 50% underestimation of those analytes (Figure 3H,I). Presumably, the durability of succinyl-CoA and propionyl-CoA analysis would be improved by use of their corresponding stable-isotope-labeled internal standards. Nevertheless, all nucleotides and short-chain acyl-CoAs, including succinyl-CoA and propionyl-CoA, could be accurately quantified for 20 days when acidified liver extracts were stored at −80 °C.

Accurate Determination of Tissue Energy Status by Snap-Freezing Tissue Samples. Although these analytes degrade in hours or days in extracts, many have half-lives on the order of seconds in tissue. As illustrated in Figure 4A, dramatic fluctuations in metabolites and cofactors related to energy metabolism are caused by ischemia (low blood flow) and hypoxia (low oxygen) during momentary delays between dissecting and freezing tissue.[31,32] Acute hypoxia inhibits ATP synthesis and NADH oxidation in mitochondrial respiration. Rapid drops in ATP and NAD^+ and accumulation of ADP, AMP, and NADH stimulate anaerobic glycolysis and rapidly inhibit acetyl-CoA and malonyl-CoA formation. These conditions cause a reduced cellular redox state (NADH/NAD^+) and accumulation of lactate, loss of pyruvate, and similar shifts in redox pairs of the TCA cycle (Figure 4A). A 10 s delay between dissection and freezing of liver tissue was sufficient to cause inaccurate measurements of lactate, pyruvate, and TCA-cycle intermediates (Figure S4). In fact, alteration of respiration or blood flow for any reason during tissue collection (anesthesia, oxygenation, euthanasia in animal models by exanguination or cervical dislocation, etc.) will cause similar shifts in metabolism with varying rapidity. For example, the order of tissue collection also impacts metabolite levels, particularly when there is significant blood loss. We dissected liver tissue from mice either immediately or after various amount of time (27–270 s) of hypovolemic ischemia (~1 mL blood collection). There was a significant decrease in ATP and a rise in AMP, demonstrating a loss of energy charge in the tissue (Figure 4B), which dropped exponentially following blood loss (Figure 4C). Although NAD^+ was unchanged, NADH increased, and the NAD^+/NADH ratio declined (Figure 4D) confirming a reduced cellular redox state during ischemia. Acyl-CoA concentrations generally decreased, except for those of propionyl-CoA, which increased (Figure 4E). These data demonstrate that blood loss during tissue collection induces rapid changes in metabolite levels, and suggests that it will be difficult to obtain accurate metabolomic analyses on multiple-tissue dissections. Hence, consideration should be given to prioritize the order of tissue collection, and allow for independent cohorts when blood loss cannot be avoided between organ collection (e.g., heart, liver, kidney, etc.).

CONCLUSIONS

An HPLC-ESI-MS/MS method was developed for simultaneous determination of nucleotides and short-chain acyl-CoAs in liver tissue. Using ion-pairing LC-MS/MS, reasonable retention times and resolutions for the analytes were achieved. To ensure high specificity, quantification was performed in MRM mode with stable isotopes as internal standards. The method was applied to the simultaneous determination of ATP, ADP, AMP, NAD^+, NADH, acetyl-CoA, malonyl-CoA, propionyl-CoA, and succinyl-CoA in mouse liver tissue. The

DOI: 10.1021/acs.analchem.9b00217
Anal. Chem. 2019, 91, 5881–5887

method is likely generalizable to other analytes in these classes of metabolites. For example, during revision of this article, we found that the method could be used to detect free CoA and GTP in liver extracts (Figure S5). The method detected hypoxia-induced changes in most analytes when tissue was collected after blood loss. This finding is not unique to the method and indicates that care should be taken in interpreting metabolomic data when multiple organs are sampled.

■ ASSOCIATED CONTENT

Supporting Information

The Supporting Information is available free of charge on the ACS Publications website at DOI: 10.1021/acs.analchem.9b00217.

Supplementary methods; calibration data for various analytes; accuracy, recovery, and precision for analysis of liver tissue; intra- and interday repeatability of the tissue processing and analytical method; effect of DBAA concentration on retention times and MS signals; effects of TEA and DMHA ion-pairing reagents on chromatographic peak shapes for nucleotides; MRM chromatograms; analyte-degradation profiles; effect of delayed sample freezing on organic acid levels in mouse liver tissue; and detection of free CoA and GTP (PDF)

■ AUTHOR INFORMATION

Corresponding Author

*Tel.: +1 (214) 645-2728. Fax: +1 (214) 645-2744. E-mail: shawn.burgess@utsouthwestern.edu.

ORCID

Shawn C. Burgess: 0000-0002-9586-5511

Author Contributions

X.F., S.D., and S.C.B. designed the experiments. S.D., B.K., and J.G.D. were involved in sample preparation and performed the experiments. X.F. and S.D. analyzed the data. X.F., S.D., and S.C.B drafted the manuscript, and J.G.M. edited the manuscript.

Notes

The authors declare no competing financial interest.

■ ACKNOWLEDGMENTS

The authors are grateful for support from NIH R01DK078184 (to S.C.B.), P41EB015908 (to S.C.B. and S.D.), the Robert A. Welch Foundation (I-1804, to S.C.B. and S.D.), and the UT Southwestern Center for Human Nutrition.

■ REFERENCES

(1) Hasenour, C. M.; Berglund, E. D.; Wasserman, D. H. *Mol. Cell. Endocrinol.* **2013**, *366* (2), 152−162.

(2) Anderson, K. A.; Madsen, A. S.; Olsen, C. A.; Hirschey, M. D. *Biochim. Biophys. Acta, Bioenerg.* **2017**, *1858* (12), 991−998.

(3) Qin, X.; Wang, X. *J. Pharm. Biomed. Anal.* **2018**, *158*, 280−287.

(4) Tang, D. Q.; Zou, L.; Yin, X. X.; Ong, C. N. *Mass Spectrom. Rev.* **2016**, *35* (5), 574−600.

(5) Kochanowski, N.; Blanchard, F.; Cacan, R.; Chirat, F.; Guedon, E.; Marc, A.; Goergen, J. L. *Anal. Biochem.* **2006**, *348* (2), 243−251.

(6) Nakajima, K.; Kitazume, S.; Angata, T.; Fujinawa, R.; Ohtsubo, K.; Miyoshi, E.; Taniguchi, N. *Glycobiology* **2010**, *20* (7), 865−871.

(7) Stocchi, V.; Cucchiarini, L.; Canestrari, F.; Piacentini, M. P.; Fornaini, G. *Anal. Biochem.* **1987**, *167* (1), 181−190.

(8) Giannattasio, S.; Gagliardi, S.; Samaja, M.; Marra, E. *Brain Res. Protoc.* **2003**, *10* (3), 168−174.

(9) Lazzarino, G.; Amorini, A. M.; Fazzina, G.; Vagnozzi, R.; Signoretti, S.; Donzelli, S.; Di Stasio, E.; Giardina, B.; Tavazzi, B. *Anal. Biochem.* **2003**, *322* (1), 51−59.

(10) Wu, J.; Zhang, Y.; Wiegand, R.; Wang, J.; Bepler, G.; Li, J. *J. Chromatogr. B: Anal. Technol. Biomed. Life Sci.* **2015**, *1006*, 167−178.

(11) Knee, J. M.; Rzezniczak, T. Z.; Barsch, A.; Guo, K. Z.; Merritt, T. J. *J. Chromatogr. B: Anal. Technol. Biomed. Life Sci.* **2013**, *936*, 63−73.

(12) Kamceva, T.; Bjanes, T.; Svardal, A.; Riedel, B.; Schjott, J.; Eide, T. *J. Chromatogr. B: Anal. Technol. Biomed. Life Sci.* **2015**, *1001*, 212−220.

(13) Cai, Z.; Qian, T.; Yang, M. S. *Se Pu* **2004**, *22* (4), 358−360.

(14) Cordell, R. L.; Hill, S. J.; Ortori, C. A.; Barrett, D. A. *J. Chromatogr. B: Anal. Technol. Biomed. Life Sci.* **2008**, *871* (1), 115−124.

(15) Luo, B.; Groenke, K.; Takors, R.; Wandrey, C.; Oldiges, M. *J. Chromatogr A* **2007**, *1147* (2), 153−164.

(16) Klawitter, J.; Schmitz, V.; Klawitter, J.; Leibfritz, D.; Christians, U. *Anal. Biochem.* **2007**, *365* (2), 230−239.

(17) Vela, J. E.; Olson, L. Y.; Huang, A.; Fridland, A.; Ray, A. S. *J. Chromatogr. B: Anal. Technol. Biomed. Life Sci.* **2007**, *848* (2), 335−343.

(18) Noack, H.; Kunz, W. S.; Augustin, W. *Anal. Biochem.* **1992**, *202* (1), 162−165.

(19) Sporty, J. L.; Kabir, M. M.; Turteltaub, K. W.; Ognibene, T.; Lin, S. J.; Bench, G. *J. Sep. Sci.* **2008**, *31* (18), 3202−3211.

(20) Kalhorn, T. F.; Thummel, K. E.; Nelson, S. D.; Slattery, J. T. *Anal. Biochem.* **1985**, *151* (2), 343−347.

(21) Hull-Ryde, E. A.; Lewis, W. R.; Veronee, C. D.; Lowe, J. E. *J. Chromatogr., Biomed. Appl.* **1986**, *377*, 165−174.

(22) Swierczynski, J.; Slominska, E.; Smolenski, R. T.; Mayer, D. *Pol. J. Pharmacol.* **2001**, *53* (2), 125−130.

(23) Yamada, K.; Hara, N.; Shibata, T.; Osago, H.; Tsuchiya, M. *Anal. Biochem.* **2006**, *352* (2), 282−285.

(24) Reszko, A. E.; Kasumov, T.; Comte, B.; Pierce, B. A.; David, F.; Bederman, I. R.; Deutsch, J.; Des Rosiers, C.; Brunengraber, H. *Anal. Biochem.* **2001**, *298* (1), 69−75.

(25) Minkler, P. E.; Kerner, J.; Kasumov, T.; Parland, W.; Hoppel, C. L. *Anal. Biochem.* **2006**, *352* (1), 24−32.

(26) Gilibili, R. R.; Kandaswamy, M.; Sharma, K.; Giri, S.; Rajagopal, S.; Mullangi, R. *Biomed. Chromatogr.* **2011**, *25* (12), 1352−1359.

(27) Gao, L.; Chiou, W.; Tang, H.; Cheng, X.; Camp, H. S.; Burns, D. J. *J. Chromatogr. B: Anal. Technol. Biomed. Life Sci.* **2007**, *853* (1−2), 303−313.

(28) Fung, E. N.; Cai, Z.; Burnette, T. C.; Sinhababu, A. K. *J. Chromatogr., Biomed. Appl.* **2001**, *754* (2), 285−295.

(29) Neubauer, S.; Chu, D. B.; Marx, H.; Sauer, M.; Hann, S.; Koellensperger, G. *Anal. Bioanal. Chem.* **2015**, *407* (22), 6681−6688.

(30) King, M. T.; Reiss, P. D.; Cornell, N. W. *Methods Enzymol.* **1988**, *166*, 70−79.

(31) Zur Nedden, S.; Eason, R.; Doney, A. S.; Frenguelli, B. G. *Anal. Biochem.* **2009**, *388* (1), 108−114.

(32) Rashidzadeh, H.; Bhadresa, S.; Good, S. S.; Larsson Cohen, M.; Gupta, K. S.; Rush, W. R. *Biol. Pharm. Bull.* **2015**, *38* (3), 380−388.

DOI: 10.1021/acs.analchem.9b00217
Anal. Chem. 2019, 91, 5881−5887